ORIGINAL ARTICLE

Study of the shear behaviour of floor diaphragms in light steel residential buildings

Nadia Baldassino, Riccardo Zandonini, Marco Zordan

Correspondence

Dr. Eng. Nadia Baldassino
Dept. Civil, Environmental and Mechanical Engineering
University of Trento
via Mesiano, 77
38123 Trento (IT)
Email: nadia.baldassino@unitn.it

Abstract

Steel housing solutions made of thin-walled cold-formed profiles (CFS) appear to be very competitive in seismic areas due to their lightweight and the associated reduced mass. This non-negligible advantage associated with the competitive costs and the ease of erection made popular this type of building solution. Aimed at investigating the potential of these structural systems, in recent years, several extensive studies of the lateral response of shear walls were carried out. On the contrary, little attention was paid to the behavior of the floor diaphragms and on their contribution to the overall building response. The University of Trento, in the framework of a wider research project aimed at the development of a residential building system made of CFS profiles, investigated the response of CFS floor systems subjected to in plane shear loading. Four types of floors characterized by two different beams systems and two different types of deck were tested in both monotonic and cyclic regime. Experimental results enabled the calibration of FE models simulating both the floor components and the whole floors. In this paper, the main features and outcomes of the tests and of the numerical analyses are presented and discussed.

Keywords

Light steel residential buildings, Cold-formed thin-walled profiles, Floor diaphragms, Full-scale tests, Numerical models.

1 Introduction

The use of housing systems made of cold formed steel profiles (CFS) is recently spreading in different countries due to some features peculiar to these structural systems such as lightweight, high structural efficiency, durability, rapidity and simplicity of installation of the building equipment. The structural system is usually made up of flooring systems, walls and foundations. Vertical loads and horizontal shear forces, due to wind and earthquake, are transferred by the floors to the walls and, then, to the foundations. According, to a common design approach, structural analyses of these systems are usually carried out considering the floor acting as a rigid diaphragm. Although this hypothesis is generally acceptable and well approximates the actual behaviour of the floor, in the case of cold-formed steel based floors, it should be verified. An accurate evaluation of CFS floors response in terms of both strength and stiffness is therefore crucial for a proper structural design. At the moment, most studies on the seismic performance of cold-formed steel framed structures focused on the lateral response of shear walls [1] while quite limited are the investigations of the diaphragms and of their contribution to the overall structural seismic response. A study of the seismic performance of a full-scale cold-formed two storey framed building was recently performed [2]. The response of the main components and of the overall building were investigated allowing pointing out the complexity of the seismic response. The floors, a wood sheathed deck on cold formed steel beams, were numerically and experimentally investigated focusing on the role and on the force distribution of the connections. The comparison of design and experimental shear strength and stiffness values proved the need of an improvement of the AISI S400 Standard [3]. These preliminary studies pointed out the various aspects of the floors response and allowed identifying the key parameters affecting their performance. The development of new diaphragm solutions, such as the ones which make use of CFS profiles combined with steel deck completed with different materials, requires 'ad hoc' investigations combining experimental and numerical studies. As a contribution to this topic, a study was carried out by the University of Trento focusing on the response of CFS floor systems subjected to in plane shear loading. Four types of floors characterized by two different beams systems and two different types of deck were tested in both monotonic and cyclic regime. Experimental results enabled the calibration of FE models related both to the floor components and to the complete floors. In this paper, the main features and outcomes of the tests and of the numerical analyses are presented and discussed.

2 The experimental program

The study focused on the response of floor systems composed of a steel frame, made of CFS profiles, completed by a deck. In detail, two steel frame types and three types of deck were considered. By combining beams frames and decking, six different floor configurations

were obtained. Ten full-scale shear tests were performed investigating the in-plane floor shear response in both monotonic and cyclic regime.

2.1 The specimens

In the following, the main components of the floor systems considered are listed and described. Since each floor is a combination of one type of steel frame and one type of decking, the specimens were identified by this combination as illustrated in Figure 1.

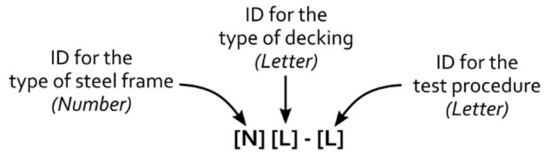

Figure 1 Nomenclature of the floor specimens

For example, the specimen named 1A-M is a floor system characterised by steel frame type 1 and a decking type A. The nomenclature is completed by the letter identifying the loading test protocol used, i.e. M in case of monotonic test and C for cyclic test.

2.1.1 The steel frames.

Two types of steel frames were considered, different for the beam types. The first type, ID 1 (Figure 2a)), has truss beams of 300 mm in height made of C-like cold formed sections [4,5]. The steel members, 100 mm height, 1.2 mm thick and made of a S 280 GD steel grade, were connected together by rivets Avdel Monobolt ϕ 6.4 mm. For each floor, 13 beams of 6 m length were used and spaced at 400 mm for a floor width of 4.8 m.

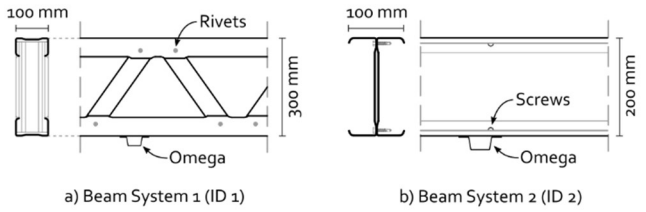

Figure 2 Beam systems used as steel frames

The second steel frame type, ID 2 (Figure 2b)), has beams obtained by coupling back-to-back cold-formed C-like sections connected together using 6.3x25 mm self-drilling screws [4, 5]. The steel profiles were 200 mm height, 1.2 mm thick and made of a S 280 GD steel grade. The floor specimens were realized with 13 coupled beams with a length of 4.5 m spaced at 400 mm for a floor width of 4.8 m. In both steel frame solutions, the beams on their bottom were transversally connected by using cold-formed omega shaped profiles, 47 mm height and 0.6 mm thick, simulating the false ceiling supports.

2.1.2 The decking

Three types of decking, conventionally named A, B and C, were investigated. All these configurations had a first layer made of steel deck sheets placed above the steel frame and connected to the beams with self-drilling screws 6.3x25 mm. Each steel deck sheet, realized with S 320 GD steel, had a height of 16 mm, a length of 2500 mm, a width of 630 mm and a thickness of 0.5 mm, and was connected to the beams along three fasteners rows. As an example, Figure 3 shows the screws pattern used to connect the single steel sheet to the truss beam steel frame (ID 1).

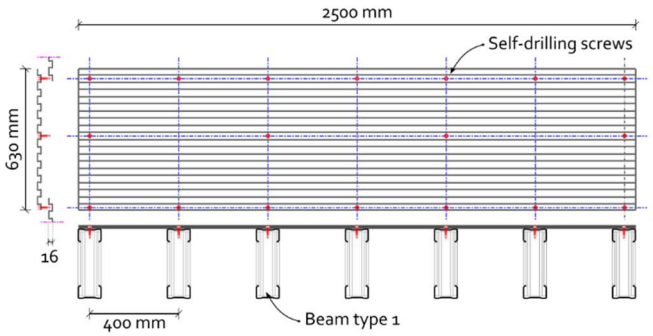

Figure 3 Pattern of connectors between the steel deck sheet to type 1 steel frame

In case of decking type A, gypsum fibre board panels were placed above the sheeting. The panels, 12.5 mm thick and with in plane dimensions of 1200x300 mm, were fastened to the steel frame with self-drilling screws. The screws used were M4.8x45 mm in specimen 1A-M, the first prepared and tested. Test results clearly show that screws M4.8x45 mm were too short to enable an effective panel-to-steel beam connection due to the uplift forces occurring when the panel deformed. Longer screws, M4.8x60 mm, were hence adopted in specimens 2A-M, 1A-C and 2A-C. In all the specimens, the screws were placed at a distance of 300 mm along the beams and at a distance of 400 mm in the orthogonal direction in order to match the beams interspace (Figure 4). Further screws were used to fix the panels along all their edges. Figure 4 shows the arrangement of the panels and the fasteners pattern of floors 1A and 2A.

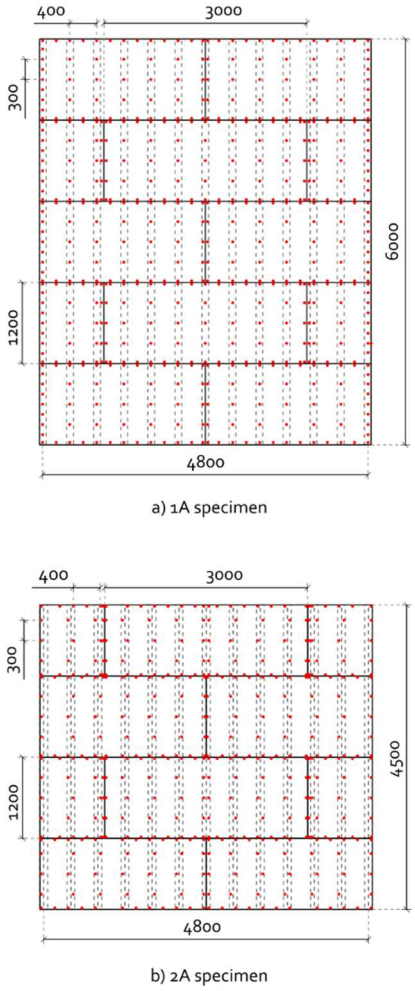

Figure 4 Decking type A and connections pattern (dimensions in mm)

The upper layer of deck assembly type B was a slab poured on the steel decking: 50 mm thick, made of light concrete LC 20/22 and reinforced with a welded mesh (Φ5 and 200x200 mm). Finally, in order to investigate the contribution of the steel deck to the in-plane floor response, in the deck assembly type C the sole steel deck was used. Therefore, combining the 2 steel frames with the 3 decking types a total of 6 floor configurations were built as reported in Figure 5.

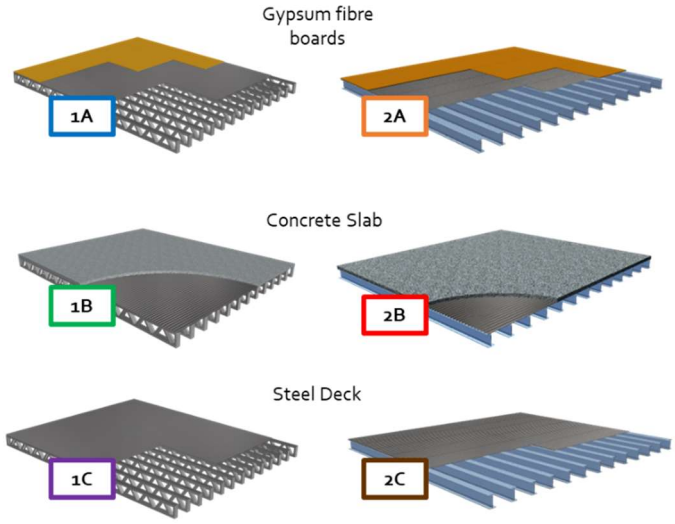

Figure 5 Deck assemblies investigated

2.2 Test set-up and instrumentation

An *ad-hoc* test set-up was designed and built (Figure 6) making possible to apply to the specimen any loading protocol under either force or displacement control.

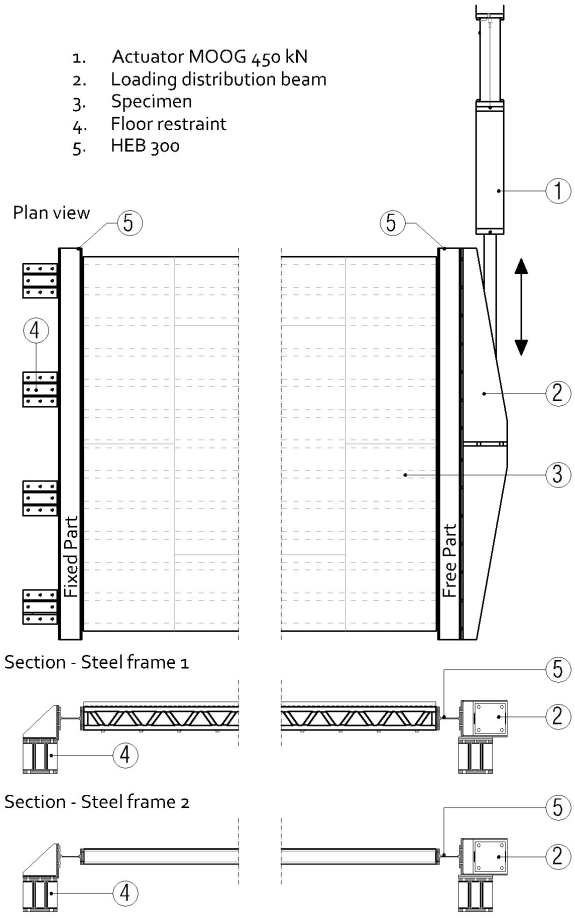

Figure 6 Test set-up

Care was taken to minimize any secondary action, and hence to approximate the in-plane shear response. The test set-up comprises of a "fixed part" and a "free part". In detail: the "fixed part" allows connecting one edge of the specimen to the strong floor of the laboratory, the "free part" at the opposite edge transfers to the specimen the shear force applied by the actuator. C section profiles connect these two opposite sides of the floor to HEB 300 S 355 steel sections. On the "fixed part" the HEB section was connected to the laboratory floor while on the "free part" the HEB section was bolted though M12 bolts class 8.8 to a loading distribution element connected to the actuator. This enables applying to the specimen an in-plane action avoiding out-of-plane displacements. In detail, the shear force was applied by means of a hydraulic MTS actuator with a stroke of 1000 mm and maximum capacity of 450 kN. All specimens were provided with wire and displacement transducers (Figure 7).

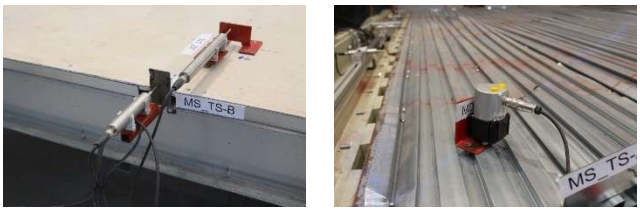

a) displacement transducer b) wire transducer

Figure 7 Instruments for displacements measurement

According to the AISI S907 [6] and ECCS prescriptions [7], the following quantities were measured: the load applied to the specimen, the horizontal floor displacement, the relative movements between the specimen and the HEB 300 beams and between the steel frame and the deck. In addition, further displacement transducers (named SLS in Figures 8a) and 9) were placed on the specimens with decking type A, in order to measure the relative displacement between the gypsum fibre board panels. Figure 9 shows the instrumentation set-up used for the 2A configuration. Since during the monotonic tests, a significant deformation of the beams ends connections was observed, during the cyclic tests, the displacement transducers labelled MT S in Figure 8b and Figure 9 were placed under the beams to more effectively characterize this behaviour.

a) SLS transducer b) MT S transducer

Figure 8 SLS and MT S transducers

2.3 Loading protocols

Monotonic and cyclic tests were performed to completely characterize the shear behaviour of the floor systems. In particular, to better catch the effect of all local phenomena, the monotonic tests were performed as a series of loading cycles with increasing amplitudes, up to the collapse. The results of the monotonic tests were then used to define the cyclic test procedure. In detail, the cyclic loading history, defined according to the ECCS recommendations [7], was based on the so-called conventional elastic limit displacement (e_y). This conventional elastic limit was defined as the abscissa of the intercept point of two tangents: i) the initial tangent (E_t) and ii) the tangent at the force-displacement curve with a slope equal to $E_t/10$, as depicted in Figure 10a).

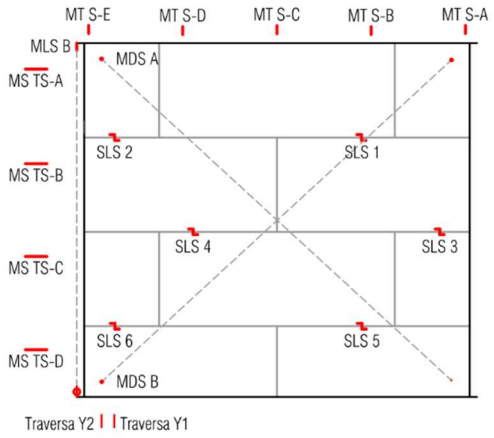

Figure 9 Instrumentation used for the 2A specimens

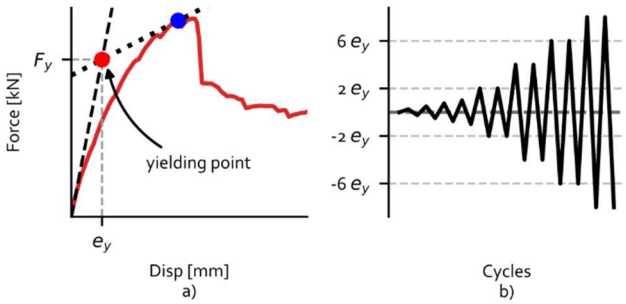

Figure 10 Cyclic loading history according to the ECCS recommendations

Once the e_y is evaluated, the cyclic procedure is defined as a function of e_y as shown in Figure 10b). By combining all the afore mentioned parameters, i.e. the steel frame type, the decking type and the loading procedure, 10 specimens were built and tested as shown in Table 1. Since the configurations with decking type C were not an actual floor solutions, they were only tested through a monotonic protocol.

Table 1 Specimens details

ID	Beam Type	Deck type	Loading procedure
1A-M	Truss	Steel sheets + gypsum fibre boards (M4.8x45 mm)	Monotonic
1B-M	Truss	Steel sheets + concrete slab	Monotonic
1C-M	Truss	Steel sheets	Monotonic
2A-M	Coupled	Steel sheets + gypsum fibre boards (M4.8x60 mm)	Monotonic
2B-M	Coupled	Steel sheets + concrete slab	Monotonic
2C-M	Coupled	Steel sheets	Monotonic
1A-C	Truss	Steel sheets + gypsum fibre boards (M4.8x60 mm)	Cyclic
1B-C	Truss	Steel sheets + concrete slab	Cyclic
2A-C	Coupled	Steel sheets + gypsum fibre boards (M4.8x60 mm)	Cyclic
2B-C	Coupled	Steel sheets + concrete slab	Cyclic

2.4 Test results

The main results of both monotonic and cyclic tests are presented and discussed in the following.

2.4.1 Monotonic tests

The results of the monotonic tests are presented in Figure 11 and Figure 12: Figure 11 shows the force-displacement curves of each monotonic test while Figure 12 compares the force-displacement envelopes by grouping the results on the basis of the beams system. The displacement is the relative displacement, in the loading direction, between the loading distribution beam and the HEB 300 beam of the fixed part.

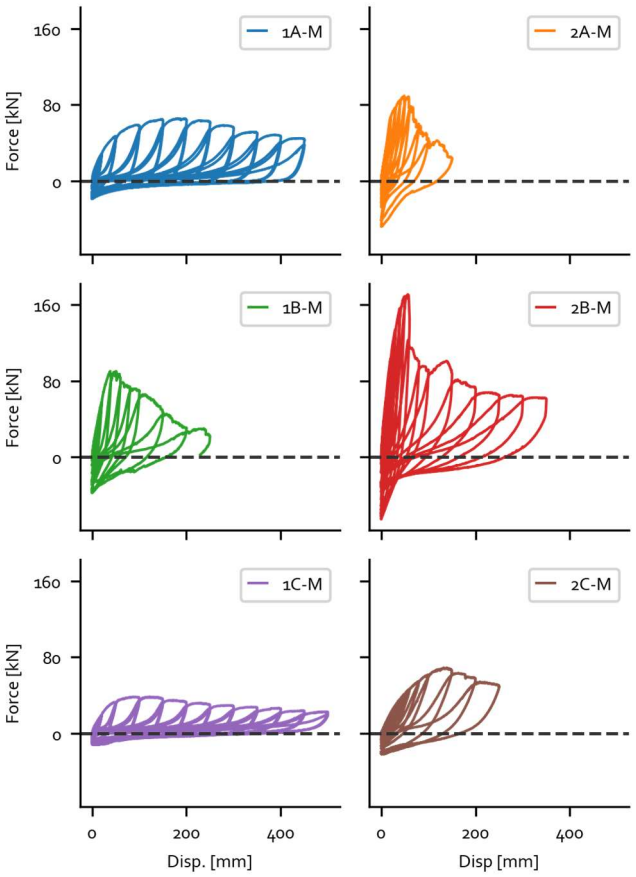

Figure 11 Monotonic tests: force-displacement curves

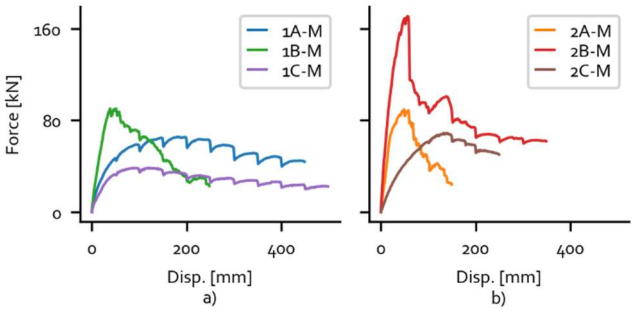

Figure 12 Envelopes curves

It is apparent that the configurations with the concrete slab (type B decking) do possess higher stiffness and strength than the ones with gypsum fibre boards (type A decking). The configurations with the sole steel deck (type C decking) showed good levels of resistance even if lower than the other decking solutions: the steel sheeting provides a non-negligible contribution to the in-plane response of

the floor. In particular, the tests pointed out the high deformation capacity of these configurations due mainly to the bearing affecting the connections.

The bearing phenomena was mainly observed in test 1C-M, as reported in Figure 13a), causing the sliding of the steel sheets (Figure 13b)).

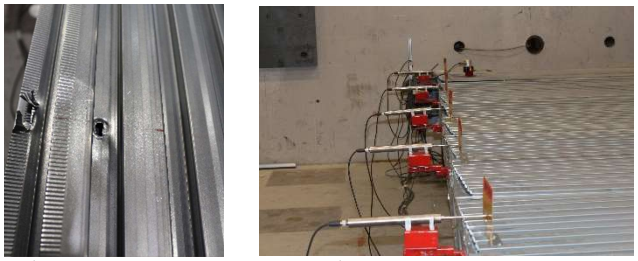

a) bearing phenomena b) sliding of steel deck sheets

Figure 13 Failure mechanisms observed in test 1C-M

On the contrary, buckling and post-buckling phenomena were mainly observed in the test 2C-M (Figure 14). In particular, Figure 14b) shows the uplift of the steel sheets which resulted in pull-through phenomena of the connectors. This behaviour was not observed in decking types A and B due to the restraint effect to the vertical displacement provided by the gypsum fibre panels and by the concrete slab.

a) b)

Figure 14 Failure mechanisms observed in test 2C-M

Tests 1A-M and 2A-M showed similar failure modes: failure of the panel-to-beam connections (Figures 15a) and 15d)), stress concentration at the floors edges and corners and high deformations and failure of the connections at the ends of the beams (Figure 15c)) In particular, the failure of the panel-to-beam connections led to the sliding of the panels as shown in Figure 15b).

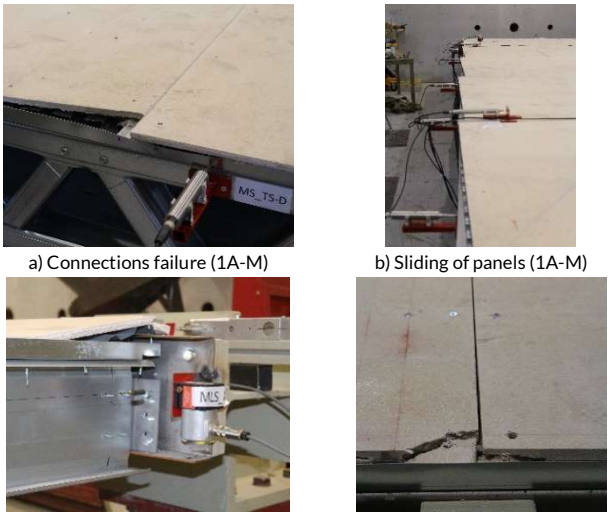

a) Connections failure (1A-M) b) Sliding of panels (1A-M)

c) Beam end connection failure (2A-M) d) Connection failure (2A-M)

Figure 15 Failure mechanisms observed in the specimen with A decking

Furthermore, results of test 1A-M, which exhibited lower resistance but greater deformation capacity than the 2A-M, were primarily caused by the 'weakness' of the panel-to-frame connections which do not effectively connect the steel sheets to the beams. As previously reported, such a behaviour determined the adoption of longer screws (M4.8x60 mm vs M4.8X45 mm). As to the floors with the concrete slab (tests 1B-M and 2B-M), the global collapse was primarily caused by the stress concentrations and the associated failure of the connections at the ends of the external beams (Figure 16a) and Figure 16b)). Furthermore, important flexural-torsional deformations were observed in the coupled beams of specimen 2A. (Figure 16c)). During the tests, the failure of the connections between the steel decking and the beams made the concrete slab acting almost independently as shown in Figure 16d).

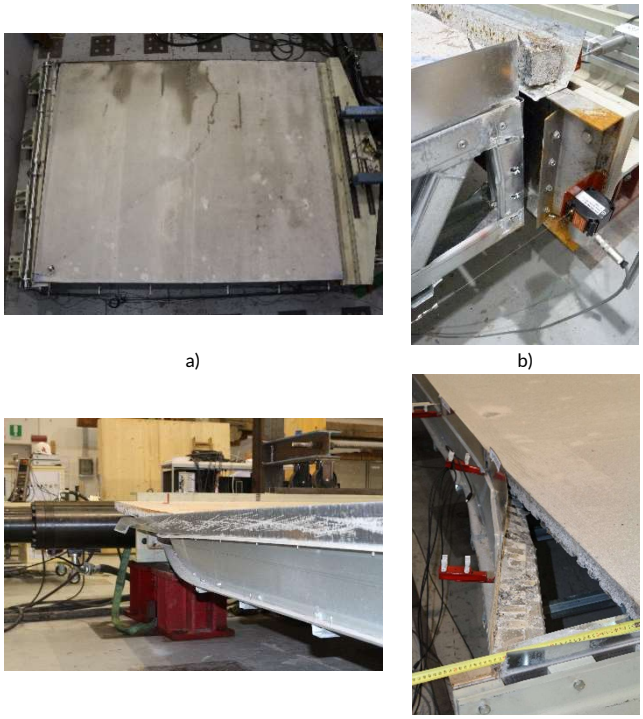

a) b)

c) d)

Figure 16 Failure mechanisms observed in specimens with decking type B

2.4.2 Cyclic Tests

Figure 17 shows the results of the cyclic tests in terms of force-displacement curves. In the figure, the envelope curves of the monotonic tests (curves in black) are plotted for comparison. All responses are characterized by a quite remarkable pinching that governs the hysteretic responses of the floor systems. This is mainly due to the connections' behaviour: in particular, the panel-to-beam and steel deck-to-beam connections. The comparison between the monotonic envelopes and the cyclic curves shows a significant reduction in terms of strength only for the configuration 2B while the configuration 2A is more affected by stiffness degradation. On the contrary, the cyclic response of specimen 1B was quite similar to the monotonic one up to a displacement of 100 mm. After that, the influence of the cyclic procedure became apparent.

The difference between monotonic ad cyclic responses of specimen 1A is associated with the different screws' length adopted for the panel-to-steel frame connections, with longer self-drilling screws in specimen 1A-C. This factor explains the substantial differences of the response in the first part of the tests: the stiffness and resistance of the monotonic test is lower due to the lack of continuity in the connections. In large displacements, the progressive failure of the connections observed in the cyclic test makes the two responses closer. As to the deformation capacity, it seems not remarkably affected by the cyclic actions.

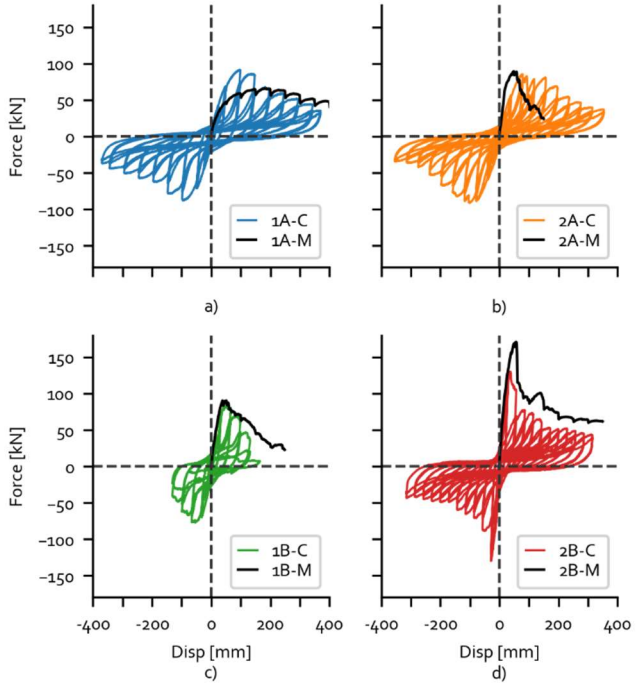

Figure 17 Results of cyclic tests

Tests 1A-C and 2A-C showed similar responses: differences in terms of strength and secant stiffness at 40% of the ultimate resistance are of 6% and 15%, respectively. For both specimens, the failure was caused by the progressive detachment of the gypsum fibre panels from the steel frame, which caused the mutual sliding between panels (Figure 18a)).

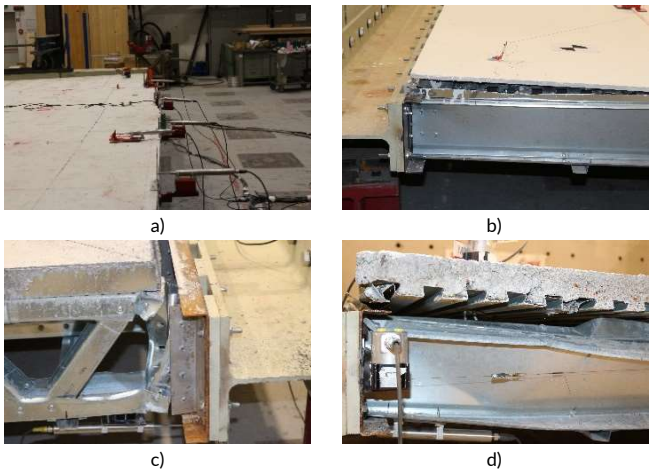

Figure 18 Failure mechanisms observed in cyclic tests

The specimen 1B-C showed the lowest deformation capacity and strength: at the fourth cycle, few connections between the steel deck and the beams failed. Nevertheless, the global collapse was caused by the failure of the connections at the ends of the beams (Figure 18 c)). The specimen 2B-C developed a collapse mechanism similar to the one observed in the monotonic test, i.e. the almost complete detachment of the concrete slab from the steel frame (Figure 18d)).

The dissipated energy is a parameter usually adopted to compare the cyclic responses. Despite the limited interest of floor system ductility for design purposes, the dissipated energy was computed in order to get a more complete appraisal of the hysteretic performance. Figure 19a) shows the total energy dissipated during the tests, while Figure 19b) and Figure 19c) report the energy dissipated cycle by cycle. As to the total energy, all floors show a similar trend: the best performance, as expected, is the one of specimen 2B-C, and the worst is that of specimen 1B-C, due to its premature collapse.

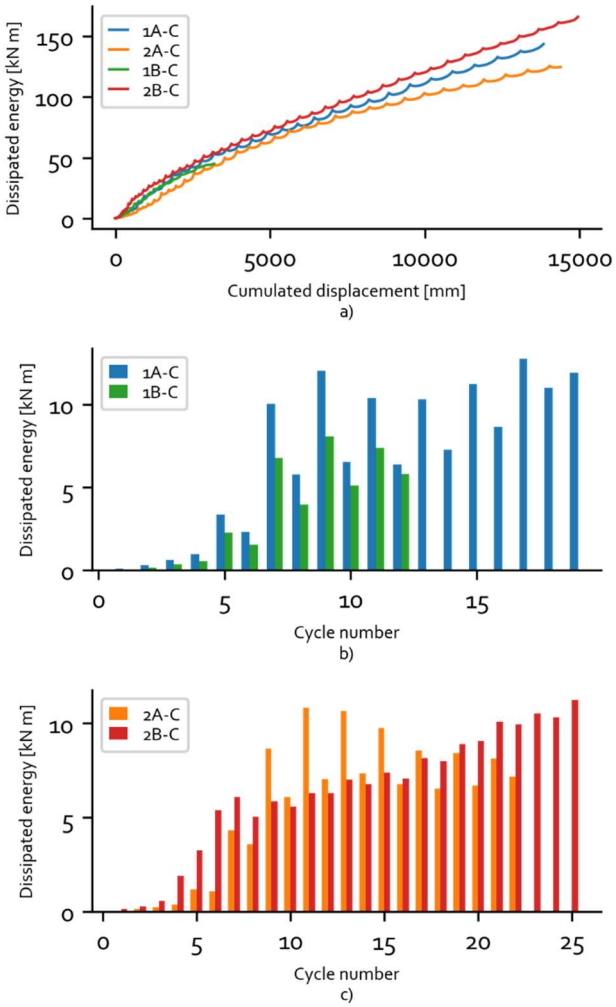

Figure 19 Energy dissipated in cyclic tests

2.4.3 *Shear stiffness and strength*

Table 2 compares the performances of all the specimens in terms of stiffness and resistance.

Table 2 Results of the tests

ID	Fmax+ [kN]	Fmax-[kN]	G'+[kN/mm]	G'- [kN/mm]
1A-M	65.63	-	1.88	-
1B-M	90.33	-	3.93	-
1C-M	38.48	-	1.29	-
2A-M	89.43	-	3.20	-
2B-M	170.78	-	5.57	-
2C-M	68.80	-	0.94	-
1A-C	91.06	88.03	2.34	2.26
1B-C	82.72	76.96	4.81	4.17
2A-C	85.21	91.20	1.64	1.64
2B-C	130.28	129.91	6.62	6.44

The diaphragm shear stiffness, G', was evaluated according to the AISI S907 [6] specifications, as:

$$G' = \frac{P_d\, a}{\Delta_d\, b} \tag{1}$$

where $P_d = 0.4\, P_{max}$ is the load associated to the 40% of the maximum load achieved in the test; "a" is the floor length in the perpendicular direction to the load; Δ_d is the shear displacement evaluated at the load P_d, while "b" is the floor depth (load direction).

The results clearly show that, in both the monotonic and the cyclic regime, the floors with the gypsum fibre boards have a lower shear stiffness than the diaphragms made with the concrete slab. This behaviour is mainly due to the higher stiffness of the concrete deck if compared to that of the gypsum fibre panels and to the slippage of the gypsum fibre panels observed during the tests.

If the attention is focused onto the steel frame type, solution 2, with beams made of coupled C sections, generally possess a higher stiffness. This could be due to the different performance in terms of lateral and torsional stiffness provided by the two beams systems.

3 Numerical analyses

The experimental results provided the background to develop numerical models since they allowed pointing out the key factors affecting the shear response of these floor typologies. At this aim, two FEM software were used: OpenSees [8] and ABAQUS [9]. OpenSees was used to set the overall models containing all the elements and components needed to simulate the behaviour of the floor systems. On the other hand, ABAQUS was used to characterise the local behaviours of the main components of the floor system such as the connections and the steel deck shear response. The models developed at this stage of the research focus on the monotonic response. In the following, the global models and the components characterization are described.

3.1 The floor-system models

With the aim to develop numerical simulations of the monotonic tests, six numerical models were developed using OpenSees. Trying to find a balance between accuracy and simplicity, a layer superposition approach was adopted. In detail, this approach models each component of the diaphragm, such as steel members, panels, steel deck and connections, into a layer. The layers are then connected to each other through rigid links. Figure 20 illustrates this approach for the model of decking type A.

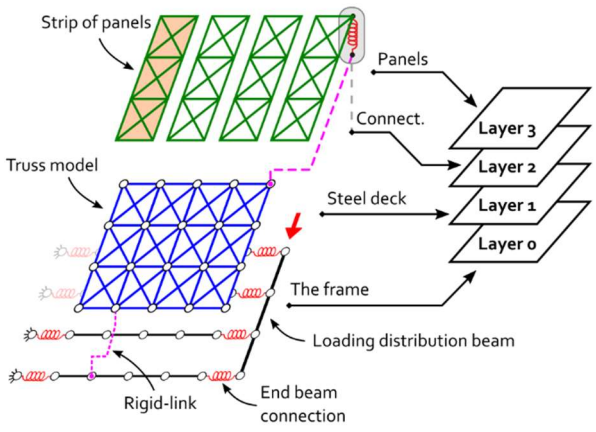

Figure 20 Layer approach used for the models with decking type A

Even though the modelling approach is the same for all the configurations, the layers differ depending on the type of floor considered as shown in Figure 21.

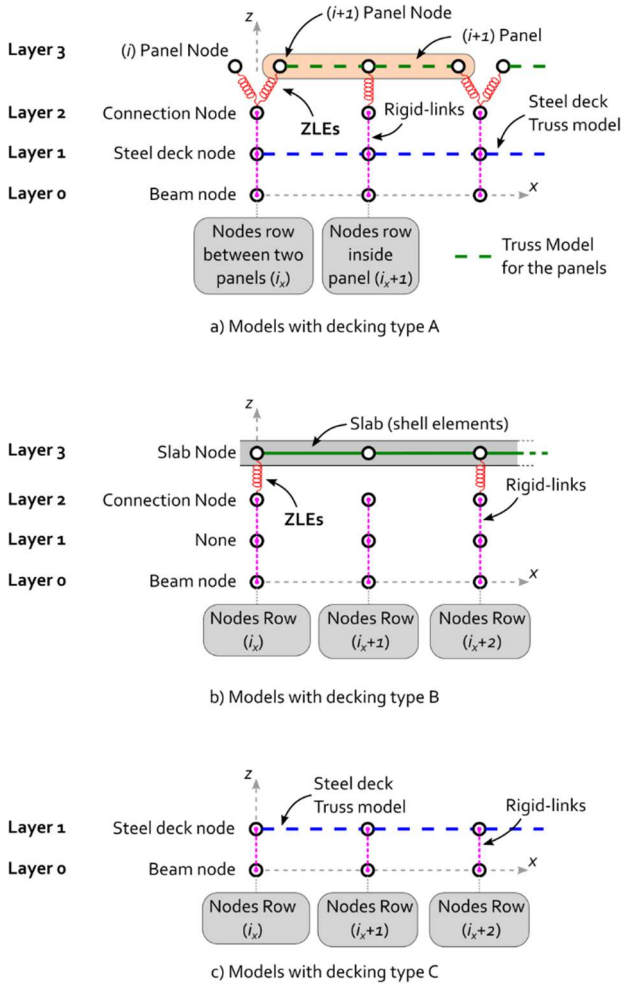

Figure 21 Layers of the models: 'vertical view' configuration

All models share the first layer (Layer 0) which simulates the steel frame and the restraints. The steel frame was modelled through elastic *dispBeamColumn* elements. The beams are connected to the external restraints using spring elements, named *zeroLength* elements (ZLE), in order to simulate the beam ends connections.

Layer 1 simulates the steel deck through a truss model numerically calibrated on the basis of the shear response of the steel deck sheets. The simplicity is the main advantage of this approach: the calibration of the single truss needs the definition of only two parameters, i.e. the shear modulus G and the mesh geometry. Therefore, the truss model enables simulating, via one-dimensional elements, the non-linear shear response exhibited by the steel deck.

Layer 2 simulates the connections between the steel frame and the decking. In particular, for the decking type A, the layer simulates the fasteners between the steel beams, or the steel deck, and the gypsum fibre panels while for the decking type B, the layer represents the connections between the steel beams and the concrete slab.

The connections were modelled through ZLEs characterized by a non-linear behaviour based on numerical simulations or on the literature, as in the following. The location pattern of the ZLEs adopted reproduces 'on average' the actual connectors arrangement. In models 1A and 2A, the seams between rows of panels were simulated through two ZLEs connected to the same node of Layer 2 (Figure 21). This enables the slippage between the panels to occur, as

experimentally observed. In models 1B and 2B, the connections pattern is based on the actual arrangement of the steel deck connections. Figure 22 shows the connections patterns in Layer 2 of models 2A and 2B.

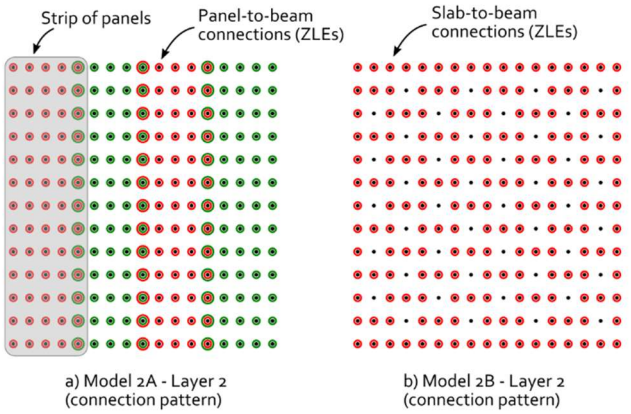

Figure 22 Layer 2: the connections patterns

Layer 3 simulates the gypsum fibre panels for configurations 1A and 2A and the concrete slab for configurations 1B and 2B. The panels of the decking type A were modelled by independent strips that in turn, were modelled through the truss model. The models 1B and 2B consider the slab as a single element modelled through elastic shell elements since the high stiffness exhibited in the experimental test. The modulus of elasticity was assumed as declared by the producer. The models 1C and 2C comprise only Layer 0 and Layer 1 which simulate the steel frame and steel deck sheets, respectively. Figure 23 and Figure 24 show the OpenSees models for configurations 1B and 2A, respectively.

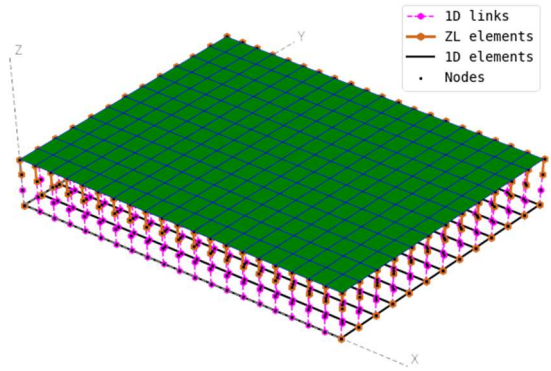

Figure 23 Schematic view of model 1B

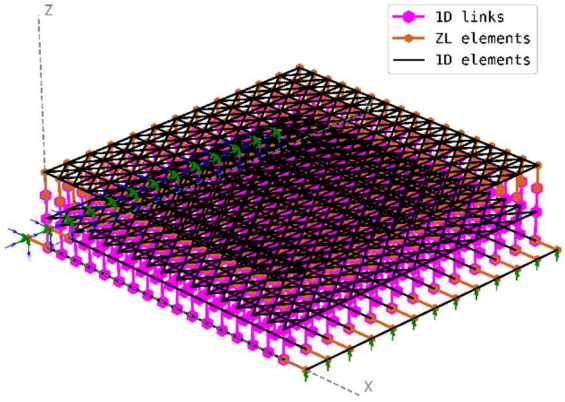

Figure 24 Schematic view of model 2A

3.2 Components modelling

The experimental tests pointed out the key role of the connections. Furthermore, the steel deck exhibited a nonlinear behaviour characterised by buckling and distortional phenomena when unrestrained by the panels or by the slab. In order to characterise these complex behaviours, ABAQUS models were set up, focusing on: i) the in-plane behaviour of the panel-to-beam connection, ii) the in-plane behaviour of concrete-slab-to-beam connection, iii) the axial, bending and torsional behaviour of beam end connection and iv) the shear behaviour of the steel deck.

Figure 25 shows the ABAQUS model of the connection between the steel flange of the beam type 2 and a gypsum fibre panel. The model was created through solid elements, taking into account a rectangular region equal to the screws spacing in both directions. The analysis, performed under displacement control, enabled obtaining a force-displacement path characterising the response of the ZLEs of the Layer 2 of model2A.

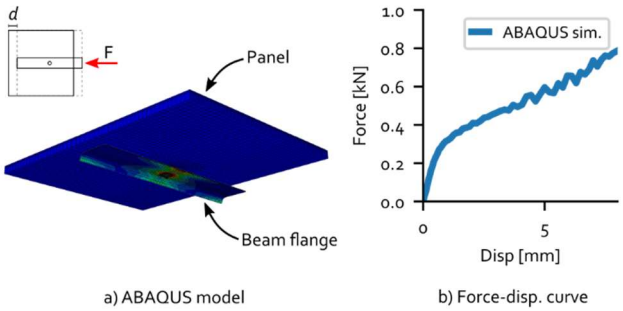

Figure 25 ABAQUS model of the panel-to-beam connection of specimen 2A

The panel-to-steel deck connections of specimen 1A-M, that differs from specimen 2A-M for the screws' length, were characterised on the basis of data provided by literature. In particular, the work of Tao at al. [10] provides the base to define the parameters of the *Pinching4 material* model, i.e. a rheological model suitable to simulate the behaviour of the connection.

The connections between the concrete slab and the steel frame were modelled in the same way as the panel-to-beam connections of model 2A: the model was created through solid elements, considering a rectangular region equal to the spacing of the steel deck-to-beams connections (Figure 3). Two analyses, in x-direction and y-direction of Figure 26a), were performed in order to obtain the force-displacement laws of the ZLEs of the OpenSees model simulating the connection's behaviour (Figure 26b)). The same procedure was adopted to simulate the connections of configuration 1B.

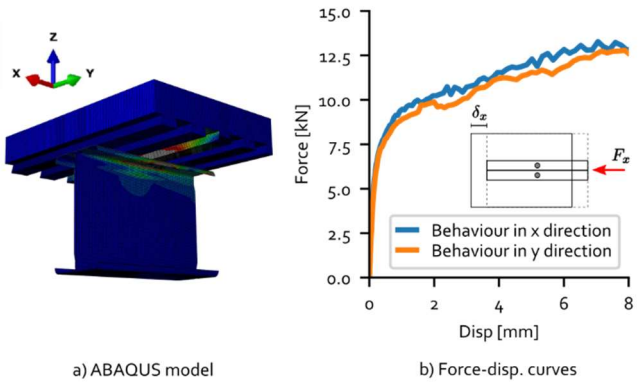

Figure 26 ABAQUS model of slab-to-beam connection of specimen 2B

Attention was paid to the model of the beam end connection of the steel frame 2 since the very high deformation experimentally observed (Figure 15c)). The model (Figure 27) takes into account the material and geometrical nonlinearities in order to properly simulate the axial, bending and torsional behaviour of that connection. The responses obtained by the ABAQUS analyses, in terms of moment-rotation and force-displacement curves, were then used to characterize the ZLEs placed at the beams ends of Layer 0. These ZLEs were defined by an axial spring in *x* direction, a rotational spring (φ_z) and a torsional spring (φ_x).

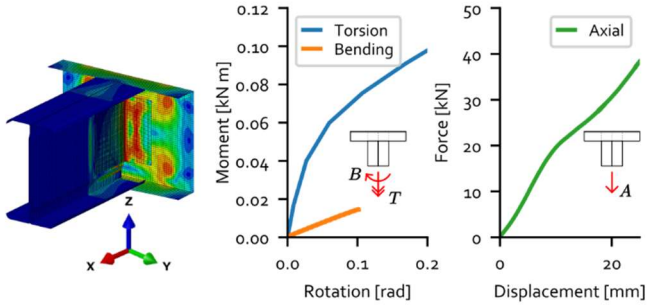

Figure 27 ABAQUS model of beam end connection of steel frame type 2

Finally, ABAQUS models (Figure 28) were created to characterise the shear response of the steel decking: two steel decking sheets were connected to a steel frame, which simulated the floor beams, taking into account the specimen screws pattern. The analysis was performed under displacement control applying a displacement in x-direction of Figure 28, i.e. the direction parallel to the long side of the steel deck sheet. Two different models, depending on the floor system, were created. In specimens1A and 2A, the gypsum fibre panels prevent the vertical displacement of the steel sheets: the vertical displacements of the steel deck (u_z displacement) are hence retrained, avoiding the sheet shear buckling (Figure 28a)). In the second model, used to characterise the truss model of specimens 1C and 2C, where the steel deck is vertically unrestrained, the vertical displacements are allowed (Figure 28b)). These analyses permitted the evaluation of the force-rotation curves, shown in Figure 28c), needed to define the non-linear transverse modulus G, used to calibrate the truss elements of Layer 1 of the OpenSees models. As expected, the analyses outcomes proved that the restrained sheet exhibits a much stiffer behaviour than the unrestrained one.

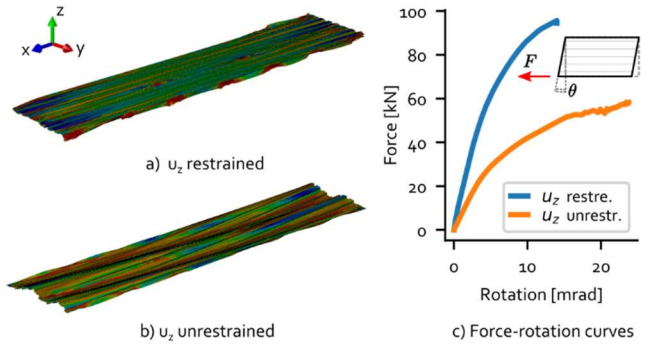

Figure 28 ABAQUS models of the steel deck sheets

3.3 Numerical vs experimental results

The results of the OpenSees analyses in terms of force-displacement curve are reported in Figure 29. The graphs compare the numerical simulation results with the monotonic experimental tests, proving the validity of the *layers approach* for the analyses of the in-plane behaviour of the diaphragms.

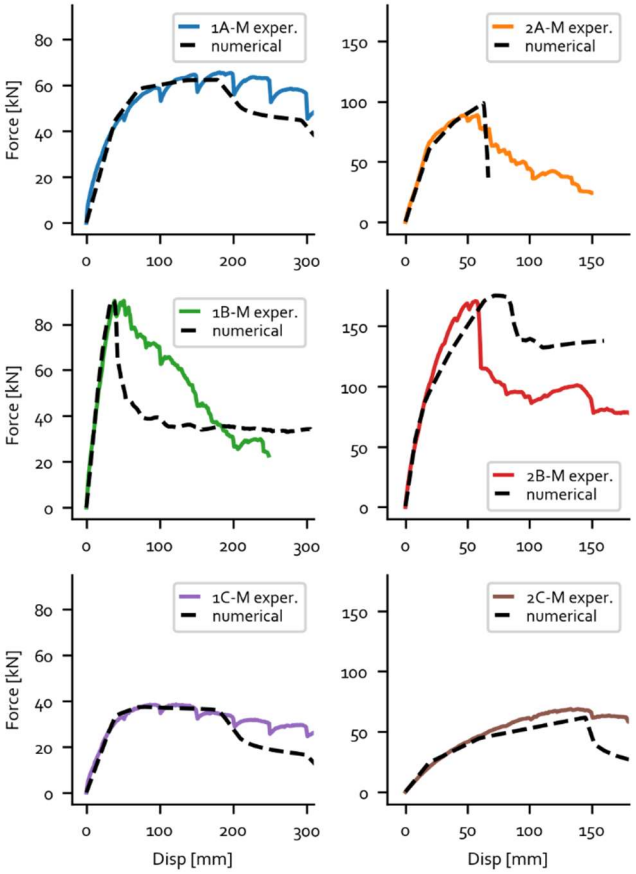

Figure 29 Numerical vs experimental results

In the figures, it is apparent the fairly good agreement between the numerical and the experimental responses up to the achievement of the maximum load. The model tends to significantly underestimate the post-peak branch of the responses. This is associated with the truss model adopted for simulating the sheeting behaviour, which is unable to catch local phenomena subsequent to the connections failure. Therefore, the model tends to underestimate the floor system ductility. However, it should be considered that floor systems are designed not to be involved in the building collapse.

4 Summary and conclusions

The study presented herein focusses on the evaluation of the in-plane responses of floor systems made of cold-formed steel frames. At this aim, experimental tests and numerical simulations were carried out.

A total of 10 full scale tests on 6 different floor system configurations were performed. The specimens differed by the steel frame and the decking solution. In particular, 2 steel frames and 3 decking solutions were adopted. The first decking solution named A was a dry solution characterized by steel deck sheets and gypsum fibre boards. The second decking solution, named B was a light concrete slab poured over a steel deck. Eventually, a last type of decking named C, with the sole steel deck placed over the steel frame was considered. The specimens were subjected to both monotonic and cyclic shear loading conditions, in accordance to the ECCS procedure [7]. The experimental programme allowed appraising the system performance in terms of both stiffness and strength, and the failure modes. As to the monotonic tests, the specimens with only a steel deck showed a good performance in terms of strength, stiffness and deformation capacity. The presence of an additional layer (concrete slab or gypsum fibre panels) results in a further non-negligible improvement of the floor shear response. As expected, the

specimens with the concrete slab showed the highest stiffness and strength. Besides, the floors characterised by the steel frame made of coupled C sections exhibited a greater stiffness than the ones characterised by the truss beams (Figure 2).

Regarding the hysteretic response, the cyclic tests pointed out a high pinching behaviour of all the configurations mainly due to the cyclic behaviour of the connections which played a key role in the mechanism of forces transfer.

Based on the experimental evidence, numerical models were then developed. The models simulated the in-plane monotonic behaviour taking into account the role of the decking and of the connections. Since the high complexity of these systems, a layer superposition approach was adopted to simulate the floor diaphragm behaviour. The overall floor models were realized using OpenSees software, whereas ABAQUS models allowed the characterisation of single components. Eventually, the comparison between the curves of the experimental tests and numerical analyses points out the satisfactory accuracy of the models. The strength and the stiffness were indeed well approximated proving the validity by layers approach.

Acknowledgments

The study was made possible by funds of the project ReLUIS 2014-2018. The Authors gratefully acknowledge Stefano Girardi and Marco Graziadei for carrying out the experimental work.

References

[1] Sharafi, P.; Mortazavi, M.; Usefi, N.; Kildashti, K.; Ronagh, H.; Samali, B. (2018) *Lateral Force Resisting Systems in Lightweight Steel Frames: Recent Research Advances*. Thin-Walled Structures **130**, 231–253.

[2] Schafer, B.W.; Ayhan, D.; Leng, J.; Liu, P.; Padilla-Llano, D.; Peterman, K.D.; Stehman, M.; Buonopane, S.G.; Eatherton, M.; Madsen, R.; Manley, B.; Moen, C.D.; Nakata, N.; Rogers, C.; Yu, C. (2016) *Seismic Response and Engineering of Cold-formed Steel Framed Buildings*. Structures **8**, 197-212.

[3] AISI S400 (2015) *North American specification for seismic design of old-formed steel structural systems*, Washington DC: America Iron and Steel Institute.

[4] ReLUIS-DPC 2014-2018 – Prodotto 1 (2016) *Sperimentazione su sistemi di piano realizzati con profili di acciaio formati a freddo*. Unità di Trento.

[5] ReLUIS-DPC 2014-2018 – Prodotto 1 (2017) *Sperimentazione su sistemi di piano realizzati con profili di acciaio formati a freddo*. Trento: Unità di Trento.

[6] AISI S907-2013 (2013) *Test Standard for Cantilever Test Method for Cold-Formed Steel Diaphragms*. Washington DC: American Iron and steel Institute.

[7] ECCS (1986) *Recommended Testing Procedure for Assessing the Behaviour of Structural Steel Elements under Cyclic Loads*, Publication P045. Brussels: European Convention for Constructional Steelworks.

[8] OpenSees Command language Manual, http://opensees.berkeley.edu/wiki/index.php/Command_Manual

[9] Abaqus 2016 Online Documentation, http://50.16.225.63/v2016/

[10] Tao, F.; Chatterjee, A.; Moen, C.D. (2016) *Monotonic and Cyclic Response of Single Shear CF Steel-to-Steel and Sheathing-to-Steel Connections*, Report No. CE/VPI-ST-16-01, Blacksburg, VA: Virginia Tech.